Nuclear Instruments and Methods in Physics Research A 817 (2016) 35–41

Contents lists available at ScienceDirect

Nuclear Instruments and Methods in Physics Research A

journal homepage: www.elsevier.com/locate/nima

First results from the new double velocity–double energy spectrometer VERDI

M.O. Frégeau, S. Oberstedt *, Th. Gamboni, W. Geerts, F.-J. Hambsch, M. Vidali

European Commission, Joint Research Centre, Institute for Reference Materials and Measurements (IRMM), Retieseweg 111, 2440 Geel, Belgium

ARTICLE INFO

Article history:
Received 23 December 2015
Received in revised form
3 February 2016
Accepted 3 February 2016
Available online 9 February 2016

Keywords:
Fission fragment mass yield
2E-2v method
Time of flight
Neutron multiplicity
$\nu(A)$

ABSTRACT

The VERDI spectrometer (VElocity foR Direct mass Identification) is a two arm time-of-flight spectrometer built at the European Commission Joint Research Centre IRMM. It determines fragment masses and kinetic energy distributions produced in nuclear fission by means of the double velocity and double energy (2v–2E) method. The simultaneous measurement of pre- and post neutron fragment characteristics allows studying the share of excitation energy between the two fragments. In particular, the evolution of fission modes and neutron multiplicity may be studied as a function of the available excitation energy. Both topics are of great importance for the development of models used in the evaluation of nuclear data, and also have important implications for the fundamental understanding of the fission process. The development of VERDI focus on maximum geometrical efficiency while striving for highest possible mass resolution. An innovative transmission start detector, using electrons ejected from the target itself, was developed. Stop signal and kinetic energy of both fragments are provided by two arrays of silicon detectors. The present design provides about 200 times higher geometrical efficiency than that of the famous COSI FAN TUTTE spectrometer [Nuclear Instruments and Methods in Physics Research 219 (1984) 569]. We report about a commissioning experiment of the VERDI spectrometer, present first results from a 2v-2E measurement of ^{252}Cf spontaneous fission and discuss the potential of this instrument to contribute to the investigation prompt fission neutron characteristics as a function of fission fragment properties.

1. Introduction

Nowadays, in nuclear fission research the focus is directed on the one hand towards the precise assessment of fragment yields relevant for the future disposal concepts for nuclear waste and delayed neutron emission. On the other hand, in view of Generation IV nuclear energy devices based on a fast-neutron spectrum, we need to better understand, how the additional excitation energy, imported by the fast neutrons, is shared between the two nascent fragments. The latter manifests itself through an enhanced prompt neutron multiplicity, which has important consequences on the criticality of such a fast-spectrum reactor. In Refs. [1,2] the authors show that the surplus of excitation energy leads to an enhanced multiplicity for heavy fragments only. Although the data are pretty obvious in the case of fast-neutron induced fission on ^{237}Np, this intriguing observation is much less evident for the target isotope ^{235}U. Further investigations with better counting statistics are needed not only for ^{235}U but also for ^{238}U and ^{239}Pu, the principal constituents of the fuel for the contemplated fast-spectrum reactors.

As shown in the just mentioned references a simultaneous assessment of both pre-neutron and post-neutron fragment masses provides an indirect information about the prompt neutron multiplicity. In this way, a study of the neutron multiplicity as a function of fragment mass, total-kinetic energy and incident neutron energy, which relates to the total excitation energy of the compound nucleus, is possible. Those correlation data are valuable input for models attempting to describe the nuclear de-excitation process in fission fragments, i.e. in very neutron-rich isotopes. Straightforwardly, it is the simultaneous measurement of the velocity and kinetic energy of both fission fragments that provides the needed information about pre- and post-neutron fragment mass.

Several attempts were made in the past to build velocity-energy spectrometers, amongst which was COSI FAN TUTTE, which operated at the high-flux reactor of the Institute Laue-Langevin in the 1980s [3]. COSI FAN TUTTE measured the time-of-flight (TOF) of the fragments with a pair of micro-channel plate detectors. In conjunction with an ionization chamber it achieved an outstanding post-neutron mass resolution, ΔA of at least 0.7 for light fission fragments ($A < 130$) and allowed nuclear charge

* Corresponding author.
E-mail address: stephan.oberstedt@ec.europa.eu (S. Oberstedt).

http://dx.doi.org/10.1016/j.nima.2016.02.011

identification by means of Bragg-curve analysis. The very small geometrical efficiency of less than $3.5\times\ 10^{-5}$ made a simultaneous measurement of both non-collinear fragments very inefficient. Key experiments were performed on thermal-neutron induced fission on e.g. ^{229}Th [4,5], ^{239}Pu [5,6], ^{232}U [5] and on ^{241}Pu [7]. The spectrometer is no longer operational.

Later similar instruments were built using e.g. thin plastic scintillation foils as fission time trigger and surface barrier detectors for TOF and energy measurements [8]. The geometrical efficiency reached just less than 0.2%. The reported timing resolution is 500 ps and no post-neutron fragment distributions are published.

The still existing need for precise fission yield data for minor actinides as well as its dependence on the incoming neutron energy triggered the development of new double velocity–double energy (2v–2E) spectrometers. Very recently a single (v,E) version of such a spectrometer was presented [9]. The design follows essentially the ideas brought forward by COSI FAN TUTTE using pairs of micro-channel plates for TOF measurements restricting the geometrical efficiency. From the information given the efficiency appears not larger than 0.1%.

At the European Commission Joint Research Centre IRMM TOF spectrometer based on the 2v-2E technique, VERDI (VElocity foR Direct particle Identification), is being developed aiming at the maximum geometrical efficiency at best possible mass resolution. The contemplated mass resolving power is $A/\Delta A\approx 130$. However, in a first step $A/\Delta A > 80$ would allow already investigating prompt neutron correlations with fission fragment characteristics. In order to approach the specification, an innovative fission trigger design was developed. In the following VERDI is presented and the different constituents described in detail. The characterization of the spectrometer and the necessary calibration procedures are outlined, and first results from a commissioning experiment on spontaneous fission of ^{252}Cf are presented.

2. Description of the VERDI spectrometer

Our spectrometer design aims at a geometrical efficiency close to 1% of 2π. To reach the contemplated value we use an array of silicon detectors located in a spherical mount with a radius of 500 mm. This configuration ensures that all fragments have the same flight path and a minimum spread in flight path length, $\delta L/L$, for any fission fragment trajectory. Fission fragments hit the energy detectors with an angle normal to the surface minimizing the spread in energy loss due to the detector's dead layer.

VERDI takes fission-fragment kinetic energy information with two arrays of silicon detectors located on both sides of the active target. They are positioned in pairs in such a way that both fragments are detected simultaneously. Up to 32 circular silicon detectors, with an area of 450 mm^2, can be placed at the end of each TOF section of VERDI adding for a total geometrical efficiency of 0.915% of 2π (see Fig. 1).

However, the key to this large detection efficiency is the innovative design of our fission start trigger. Until now those devices are built upon using ultra-fast micro-channel plates (MCP), which detect electrons ejected by fission fragments when passing through an emitter foil. Since this foil has to be as thin as possible to avoid undesired large energy loss and straggling, the open diameter of such a foil is limited. The simultaneous use of a pair of MCP detectors are the reason for the low geometrical efficiency of previous designs.

Our design is based on the use of electrons ejected from the ultra thin backing of the actinide deposit. Those backings can be produced from nickel foils with a thickness of 250 nm or from polyimide foils with a thickness smaller than 220 nm,

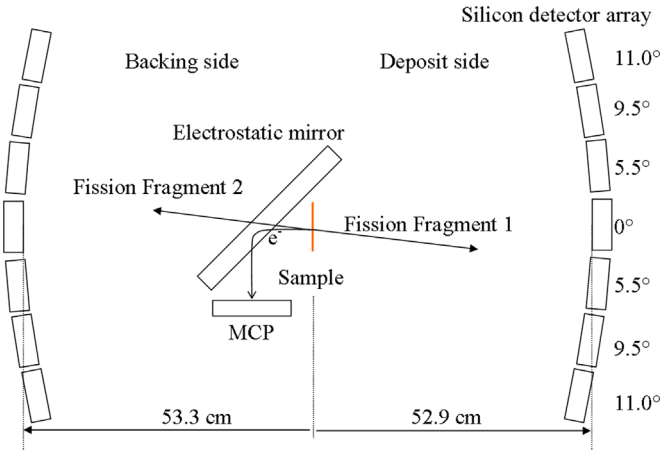

Fig. 1. VERDI diagram showing the central FIssion Electron Time-of-flight Start (FIETS) detector and the two energy detector spheres at the end of each time-of-flight section (not to scale). Fragments can be detected by one of the silicon detector pairs, while the electrons, emitted by the target, are deflected by the electrostatic mirror into the direction of the micro-channel plate (MCP) detector.

corresponding to a typical energy loss for heavy fission fragments around 5 MeV. The corresponding open cone of such a MCP assembly allows fission fragments to reach the array of silicon detectors, leading to a geometrical efficiency about 200 times larger than that of the COSI FAN TUTTE spectrometer and still a factor of 10 larger than that of SPIDER [9].

The complete characterization of VERDI was performed with a ^{252}Cf source allowing us to benchmark its performance relative to the well known characteristic of fission fragments from ^{252}Cf(sf). The source, with an activity around 2000 fission/s at the moment of the characterization, was deposited on a nickel film of 250 nm thickness. The initial source was mainly composed of ^{252}Cf, but contained also a significant amount of ^{251}Cf, ^{250}Cf, ^{249}Cf and their decay products.

2.1. The fission electron time-of-flight start detector FIETS

The FIssion Electron Time-of-flight Start (FIETS) detector has been designed to provide us with the time-zero signal for the emission of fission fragments. It uses a micro-channel plate (MCP) detector to detected the electrons, which are emitted directly from the source under the influence of the ejected fission fragments. This particular design maximizes the open angle of emission while minimizing energy losses suffered by the fragment by omitting an extra emission foil in the trajectory of the fragment. Due to the relatively small dimension of the deposit with respect to the total flight-path length, the origin of the fission fragment does not introduce any significant uncertainty to the flight distance. Therefore, no dedicated measurement of the position of the fission event on the sample is required. The MCP is in the so-called Chevron configuration with an aspect ratio 60:1. The pore size is equal to 25 μm and the centre-to-centre distance 32 μm. The front side of the MCP is at ground level to avoid a residual electric field between the MCP and the electrostatic mirror. A bias of + 2300 V is applied to the back side of the MCP. The first delay line is held at the same voltage. The second delay line is set to + 2336 V. The MCP anode is kept at + 2356 V. The signal taken from the backside of the MCP is used to determine the fission time zero. The FIETS assembly is operated with dedicated electronics supplied by the producer [10], and provides, beside the timing information, also position information by means of the delay line method. The position information is only used for controlling the proper adjustment of the different components of the FIETS detector.

Electrons are first accelerated to 3 keV by an electric potential held between the target and a grid. The distance between the grid and the source is 4 mm. In order to avoid deformation, or even rupture of the ultra-thin target foil by the electric field, a similar grid is placed symmetrically on the other side of the target. Electrons are then deflected by a pair of grids lying at 45° relative to the detector axis, acting as an electrostatic mirror (see Fig. 2). The grids are made from 50 μm tungsten wire separated by a pitch of 1 mm. The electrostatic mirror has a transmission of 90.3%. When combined with the acceleration grid, the total transmission is then 85.7%.

The high voltage between the mirror grids was set to satisfy the condition of isochronous transport according to the equation derived by Kosev et al. [11]. Fulfillment of this equation ensures that, no matter what the emission angle is, electrons emitted from the source will have the same travel time to the MCP. Minimizing the travel time spread is essential to minimize rise time variation and the associated time jitter. A signal rise time as fast as 2 ns was observed at the exit of the fast amplifier connected to the decoupling circuit of the MCP. The timing properties of the FIETS detector were determined with α-particles from a ^{241}Am source, coupled to a single-crystal diamond detector, which was fully characterized earlier [12]. The FIETS detector has an intrinsic timing resolution as good as $\sigma_{int} = 140$ ps (see Fig. 3).

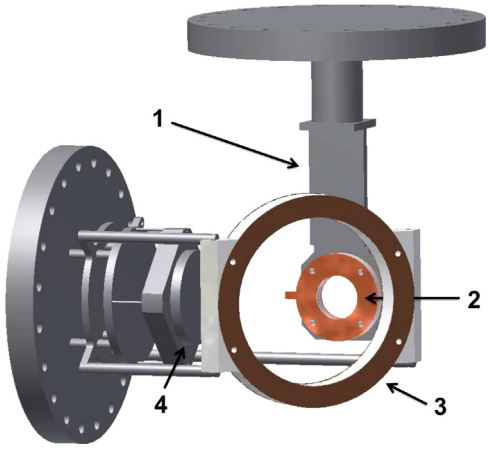

Fig. 2. Design of the FIssion Electron Time-of-flight Start (FIETS) detector, with sample holder (1) and acceleration grid (2), with the electrostatic mirror (3) and the micro-channel plate (MCP) detector (4).

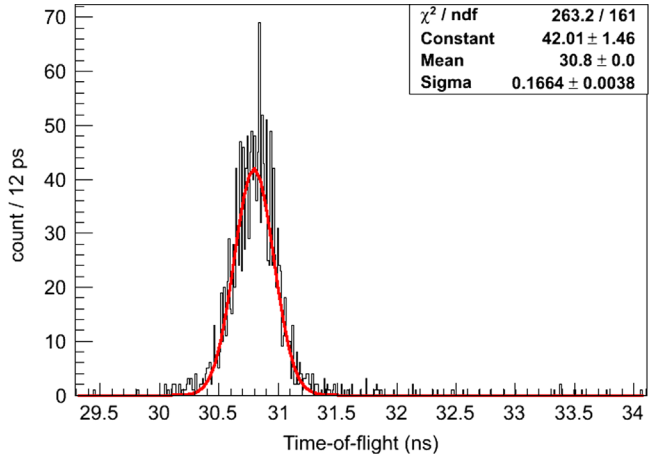

Fig. 3. Time-of-flight spectrum of an α-particle of energy $E_\alpha = 5.5$ MeV measured between the FIETS detector and a previously characterized single-crystal diamond detector; from the fit of a Gaussian function to the measured distribution the intrinsic timing resolution of the FIETS detector was determined to $\sigma_{int} = 140$ ps.

2.2. Energy and time-of-flight measurements with silicon detectors

The arrival time and the kinetic energy of the fission fragment are measured with Passivated Implanted Planar Silicon (PIPS) detectors. Such detectors have already been used during a feasibility study on VERDI with a relatively good timing resolution, but their small area (25 mm^2) severely limited the geometrical efficiency achievable [13]. Detectors with considerably larger size show a notably degraded timing resolution due to an inhomogeneity of doping across the area. To limit degradation of timing resolution Canberra produces a so-called timing optimized detector by adding an aluminum layer to the detector window. As a result a timing resolution as good as 200 ps is expected. In addition, we used neutron transmutation doped silicon material for the detector. This doping technique reduces significantly the inhomogeneities in the silicon wafer and, therefore, the variation in the signal rise time and the associated time jitter. In a dedicated experiment the timing resolution for fission fragments of such NTD silicon detectors, with an area of 450 mm^2, was determined to σ_{int}=150 ps [12].

The silicon detector signals are fed into Mesytek MSI-8 (8 channel) pre-amplifier and shaping modules [14], which provides the pulse height information together with a fast signal. The fast signal is then fed into a CAEN N843 16-channel constant fraction discriminator [15], the output of which serves as stop signal for the time-of-flight measurement.

In the following, the characteristics of our energy and TOF stop detectors will be presented along with the principle analysis applied to data obtained with a 2v–2E spectrometer like VERDI.

3. Data analysis of double velocity–double energy measurements

For the characterization of VERDI and to compute fission fragment masses it is necessary to establish an energy and time of flight calibration. In the absence of ion beams of well-defined mass and kinetic energy we used a ^{252}Cf source. The characteristics of the source are described in Section 2.

Characterization and calibration with a fission source requires a particular procedure, which will be presented in the following. In the end it also served as a commission experiment for VERDI, demonstrating the capabilities of our spectrometer.

3.1. The energy calibration

The Schmitt calibration procedure [16] was used. This mass dependent calibration procedure gives a complete calibration taking into account the energy loss of the fragment in the detector's dead layer and the pulse height defect:

$$E = (A + A' * m) * K + B + B' * m, \quad (1)$$

where E is the calibrated energy, K the ADC channel, m the fragment mass and A, A', B, B' the calibration coefficients. The coefficients are a function of the centre of each peak and of the energy measured with ion beams. Unlike Schmitt et al. our californium source could not be considered as unperturbed. Indeed, the source was about 3.4 years old and, therefore, under the effect of sputtering, the californium is assumed to be homogeneously diffused into the backing material. As a consequence the average energy from Schmitt was corrected for energy loss in the backing, and new coefficients A, A', B, B' were computed. The mass of the fragment was computed with the energy and the time of flight in an iterative procedure. The latter was found to converge within few iterations. The quality of this procedure can be appreciated in Fig. 4 in a comparison between our kinetic energy distribution and

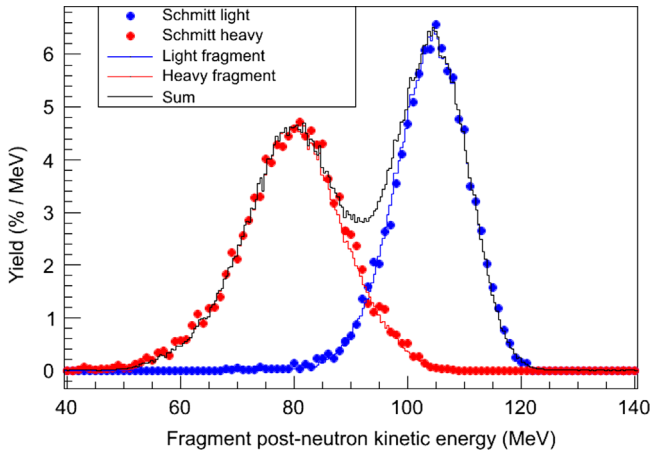

Fig. 4. Post-neutron kinetic energy of light and heavy fragment compared to results of Schmitt et al. (dots) [16].

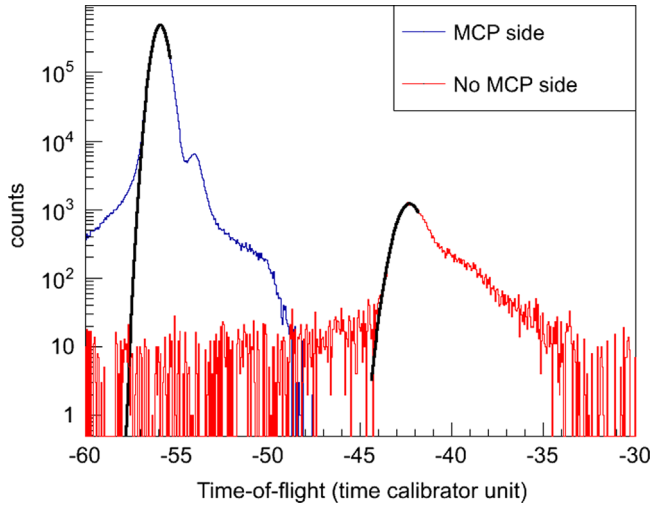

Fig. 5. Time of flight spectrum of the α particle of the californium source from both sides of VERDI. The black line is the result of a Gaussian fit used to obtain the peak position.

data from Schmitt et al. [16]. Our data are compared for light and heavy fragments separately, and both distributions show excellent agreement with data from literature [16].

The broad distribution in mass and energy of the fragments does not allow evaluating directly the energy resolution. We, therefore, rely in first order on the α particles from ^{252}Cf. However, it should be stressed that the energy of α particles, with $E_\alpha \approx 6.1$ MeV, is much smaller than fission fragment energies and, therefore, lie at the low end of the ADC's dynamical range suffering from a significant noise contribution. The observed $\Delta E/E$ (FWHM)=0.016 is imparted to the important electronic noise observed at the output of the pre-amplifier. In an experiment with a proper dynamical range for α-particles a $\Delta E/E$ (FWHM)=0.004 was observed [12]. We may assume that the energy resolution at fission fragment energies is close to this value.

3.2. Time-of-flight calibration

The absolute time of flight calibration was performed with a time calibrator for the slope, and the offset was determined by the time-of-flight measured for the α-particles of ^{252}Cf (Fig. 5). The ^{252}Cf α-peak is composed of two main unresolved peaks. Our source also contains a non-negligible amount of ^{250}Cf, which also has a significant contribution to the main peak. The energy used for this peak, and the corresponding time-of-flight, was the weighted average of the different α-particle energies. The corresponding spectrum is shown in Fig. 5 for the side with and without MCP detector.

It is to note that the calibration was much more difficult to perform on the side of the detector opposite to the MCP detector. For α-particles detected in this direction electrons are mainly emitted in the same direction as the α-particle and, therefore, they are not detected by the MCP. Still, for a small fraction of α particles emitted in the direction opposite to the MCP sufficient electrons were emitted backward and detected by the MCP. Nonetheless, the weak number of counts in this peak and the reduced timing resolution significantly limited our ability to make effective cuts in energy and time of flight to perform an optimum time-of-flight calibration.

The α particles show a reduced timing resolution of not better than 1.4 ns. As for the energy resolution, the dynamical range, complying with fission-fragment signals, leaves α particle signals notably affected by electronic noise.

3.3. Determination of the plasma-delay time

The plasma-delay time (PDT) is certainly one of the main limitation when using silicon detectors for timing purpose. We use a method close to the one used in a spectrometer using silicon detectors for time-of-flight measurements as well [1,8]. The post-neutron mass of the fragments is computed with the help of the kinetic energy measured by the silicon detectors and by conservation law.

$$m_{pre,i} = \frac{E_j^L}{E_i^L + E_j^L} M_{tot} \tag{2}$$

where $m_{pre,i,j}$ and $E_{i,j}^L$ are the pre-neutron mass and kinetic energy of the fragments in the laboratory frame of reference. The pre-neutron kinetic energy is computed assuming the neutron energy in the centre-of-mass (CM) frame and the neutron multiplicity $\nu(TKE, M_{pre})$ measured independently [17]:

$$E_{post}^L = \frac{m_{post}}{m_{pre}} E_{pre}^L + \frac{m_n}{M_{post}} E_n^{CM} - 2\sqrt{\frac{m_n E_n^{CM} E_{pre}^L}{M_{pre}}} \cos\omega_n^{CM} \tag{3}$$

neglectig the last two terms,

$$E_{pre}^L \approx \frac{m_{pre}}{m_{post}} E_{post} \tag{4}$$

The post-neutron mass can then be calculated directly by subtraction of the emitted neutrons.

$$m_{post} = m_{pre} - \nu(TKE, M_{pre}) \tag{5}$$

Knowing the mass of the fragment it is possible to compute the appropriate PDT.

$$PDT = t_{exp} - d\sqrt{\frac{m_{post}}{2E_{post}}} \tag{6}$$

Since the energy calibration uses the time-of-flight information to determine the mass dependence, the PDT correction was performed simultaneously with the energy calibration in an iterative procedure.

This procedure requires one to know a priori the neutron multiplicity. This is not a problem for ^{252}Cf(sf), but for other systems it can be much more difficult or even impossible. Also, in regards of the objective of computing prompt neutron multiplicities with VERDI, it would be highly desirable to avoid imputing this quantity in the analysis. To establish the correction without going through the later process we use the experimental scaling law between the measured velocity and the real velocity

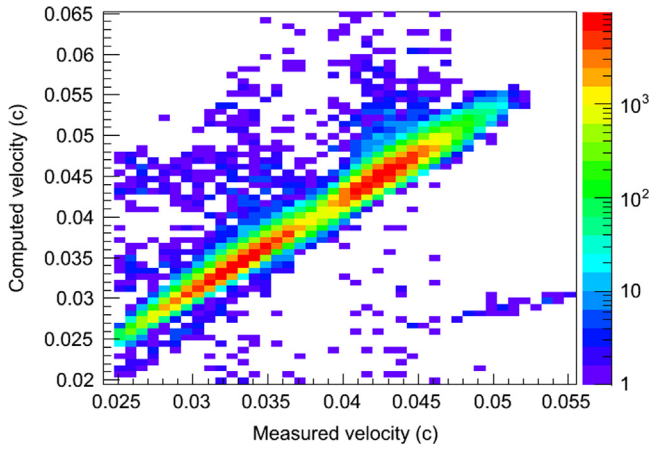

Fig. 6. Corrected velocity as a function of experimental fragment velocity. The black line is a linear fit to the data (see text for details).

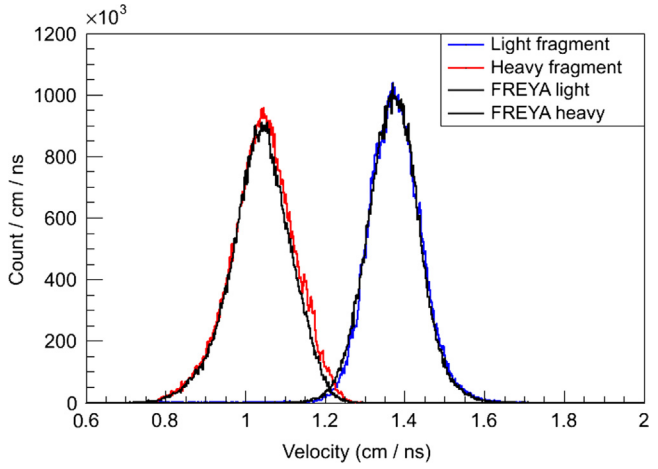

Fig. 7. Corrected velocity for light and heavy fragments compared to velocities computed with the Monte-Carlo code FREYA [19].

observed by [18]. Fig. 6 shows the velocity with the kinetic energy of the fragments as a function of the measured velocity. It was successfully fitted by a linear function. This function was later used directly for PDT correction. Note that this procedure corrects not only for PDT but also for other experimental features, which may influence the timing such as walk induced by the constant fraction discriminators and was, therefore, performed independently for each detector. The corrected velocity distribution for light and heavy fragments is depicted in Fig. 7. The distribution is compared to a velocity distribution computed with the FREYA code [19]. First of all we may conclude that both distributions are in very good agreement. The small excess and the structure on the right part of the velocity distribution of the heavy fragments still needs to be further investigated.

The width of both distributions for light fragments show perfect agreement. Since no additional broadening due to timing resolution is included in the simulations, we conclude that the timing resolution of VERDI is better than the resolution broadening induced by prompt neutron emission.

In Table 1 we compare our average velocity for light an heavy fragments with data from Schmitt et al. [16] and Whetstone [20]. The latter data represent pre-neutron velocities drawn from a double-energy measurement.

Table 1
Comparison of average light and heavy fragment velocities; the data marked with a † is pre-neutron velocities obtained from a double energy measurement.

	This work	Schmitt et al. [16]	Whetstone [20]†
$\overline{v_L}$ (cm/ns)	1.377 ± 0.004	1.383 ± 0.006	1.375 ± 0.007
$\overline{v_H}$ (cm/ns)	1.043 ± 0.005	1.036 ± 0.005	1.036 ± 0.005

3.4. Pre-neutron mass determination

The pre-neutron masses were directly determined by application of the conservation of momentum.

$$m_i = \frac{v_j}{v_i + v_j} M_{tot} \tag{7}$$

m is the fragment mass and v its velocity at scission. M_{tot} is the sum of mass of the fragments, i.e. in our case 252 u. Under the influence of the neutron emission the fragment velocity is modified. Nonetheless, under the assumption of isotropic neutron emission, the average velocity is conserved. Neutron evaporation will, therefore, induce a broadening in the mass distribution around the average value. From kinematics and non-isotropic prompt neutron emission we may not expect a pre-neutron mass resolution σ_A smaller than one mass unit.

To evaluate the effect of neutron evaporation on the pre-neutron mass resolution we computed the masses with Eq. (7) and with the fragment velocity provided to us by the code FREYA [19]. This code uses a set of experimental data to perform a Monte-Carlo sampling of fragments, prompt neutrons and gamma-rays. The resulting quantities contain, therefore, realistic correlations between fragment velocity and neutron multiplicity. The resulting distributions are shown, as a function of the total neutron multiplicity in Fig. 8. The figure also displays the spectrum summed over all neutron multiplicity gates, i.e. the spectrum which is expected to be measured, if VERDI had an infinite timing resolution. From that, pre-neutron mass distributions should not show resolved mass peaks.

The velocity of the fragments is directly computed by the procedure outlined in Section 3.3. To obtain the pre-neutron mass it is required to correct this velocity for the slowing down in the backing. This is done by computing the energy loss of the fragment in the backing and converting it into velocity loss. Once more it was assumed that the fragments come from the centre of the backing. The charge of the fragment was computed as if it has the same A/Z as ^{252}Cf. This approximation, which neglects the well-known charge polarization (see e.g. Ref. [21]) has a negligible effect on the final velocity. The resulting mass distribution is depicted in Fig. 9 along with the mass distribution measured by Hambsch et al. with the double energy method [22]. Very good correspondence between our data and that from Ref. [22] can be observed at the exception of the symmetric region where the dip is more pronounced in our data. We interpret this difference as a consequence of the superior resolution of VERDI. In Fig. 9 we observe that the symmetric region is also filled in the simulation from FREYA, but this is only the consequence of the use of the double-energy data as input data in FREYA.

3.5. Post-neutron mass determination

Post-neutron masses are computed directly from each fragment kinetic energy and corrected velocity as depicted in Figs. 4 and 7, respectively. In Fig. 10 we show the corresponding mass distributions as obtained for the deposit and the backing side, separately. Only events, where both fission fragments were detected, are shown. Relatively good agreement with the

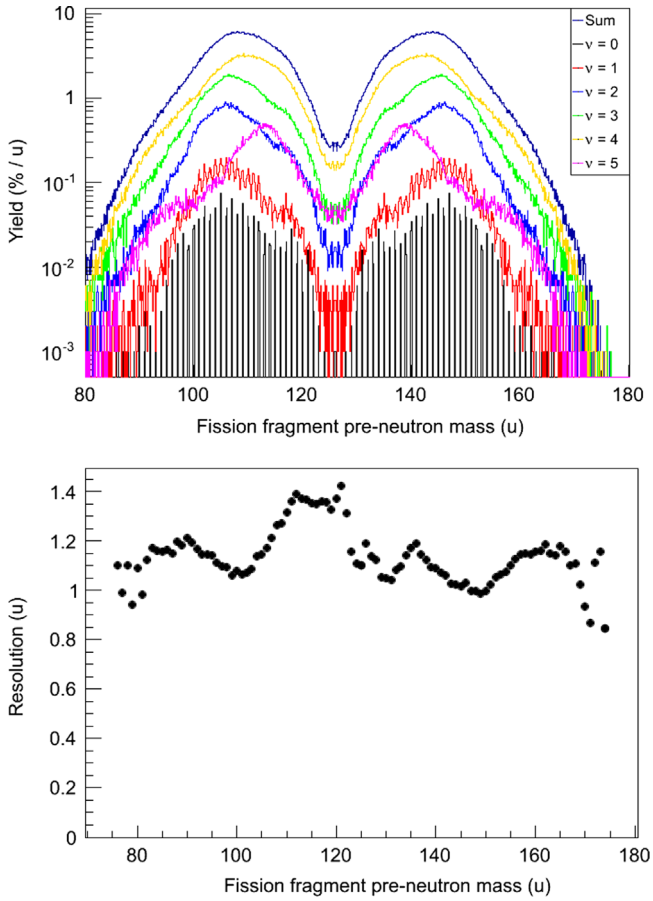

Fig. 8. Simulated fission fragment mass distributions for different assumptions of the number of prompt neutrons emitted are shown in the upper part; complete fission events generated with the computer code FREYA [19] were used to compute the effect of prompt neutron evaporation on the pre-neutron mass resolution. The lower figure depicts the resolution as a function of the fragment mass fully accounting for prompt neutron emission.

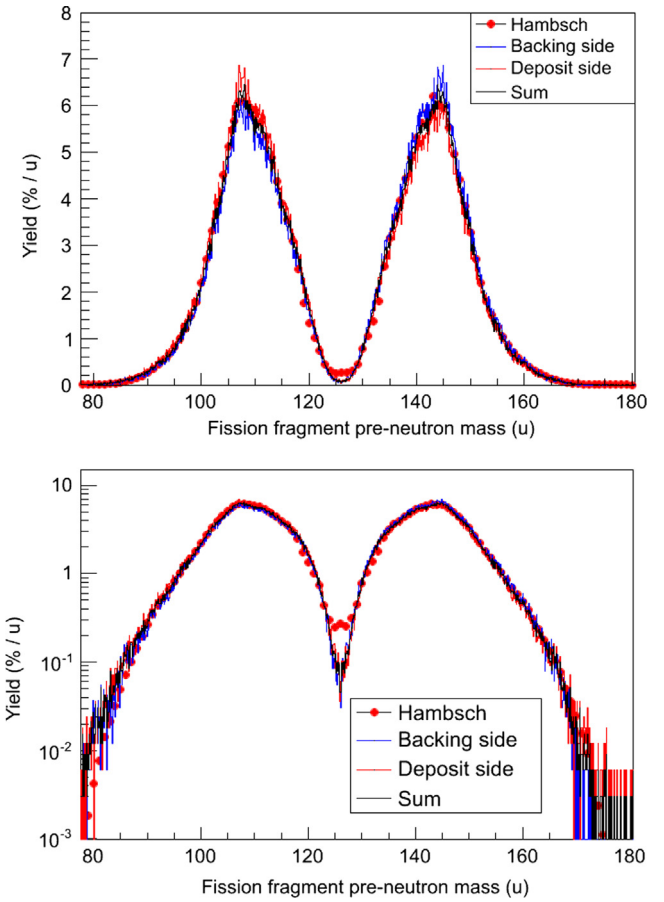

Fig. 9. Pre-neutron mass yields obtained with VERDI (full lines, see text) compared to data of Hambsch et. al. [22] (symbol) shown in linear scale (upper part) and logarithmic scale (lower part); more structure around the maximum of the distribution is visible in our data, and VERDI achieves a peak-to-valley ratio of more than 60, which is an improvement by a factor of 3 (see lower part).

evaluation of England and Rider [23] is achieved for the light fragment distribution, but the distribution of heavy fragments is broader. The England and Rider evaluation is based partially on radio-chemical data. Therefore, we compare our results also with data deduced from the double-energy measurement reported in Ref. [22] taking neutron evaporation into account, which resembles that from England and Rider. We conclude that the discrepancy is due to a deterioration of the energy resolution of the PIPS detectors at decreasing kinetic energy, most likely caused by a decreasing signal-to-noise ratio due to the electronic noise.

3.6. Neutron multiplicity

Despite the fact that the post-neutron mass resolution lies below expectation we attempt to compute the mass-dependent neutron multiplicity by simply evaluating, event-wise, the difference between pre-neutron and post-neutron mass. The corresponding average neutron multiplicity as a function of pre-neutron mass is shown in Fig. 11 and compared to the neutron multiplicity measured with a liquid-scintillator based neutron detector by Göök et al. [17]. The error bar depicts the statistical error on the average neutron multiplicity. The features of the shape of the $\nu(A)$ distribution are very well reproduced. The sharper minimum just below mass number 130 may be due to the better mass resolution. The total average multiplicity is higher by about 15%.

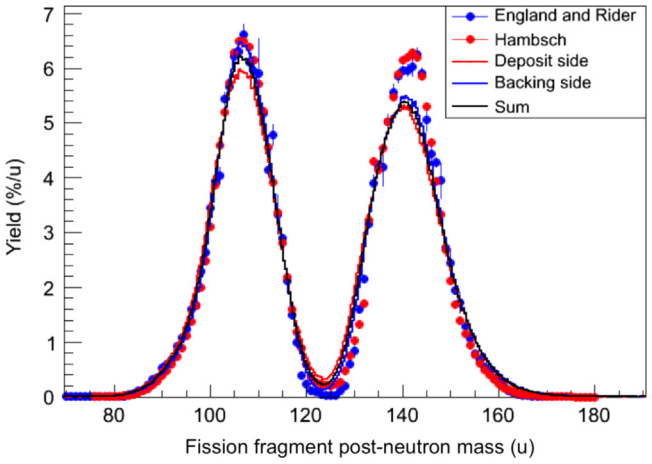

Fig. 10. Post-neutron fragment mass distribution compared to experimental data obtained with the double-energy technique [22] and to the evaluation of England and Rider [23]; our distributions are shown for both deposit and backing side separately.

4. Conclusion

We presented the new VERDI double velocity–double energy spectrometer together with first results from a commissioning experiment. A simultaneous measurement of pre-neutron and post-neutron fragment yield distributions from the spontaneous

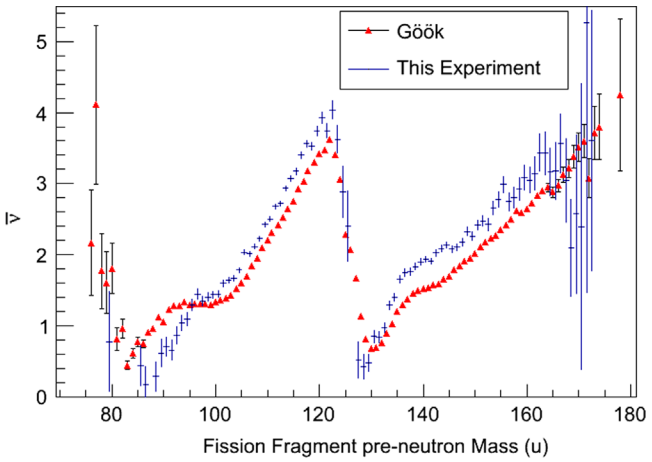

Fig. 11. Average neutron multiplicity as a function of fission fragment mass calculated from the event-wise difference of pre- and post neutron masses demonstrating the power of the VERDI spectrometer. Our data are compared with most recent data directly measured by means of the double-energy technique in conjunction with a neutron detector [17]. Both shapes of the distribution agree with each other, whereas our average total neutron multiplicity turns out to be about 15% higher than the reference value (see text for details).

fission of ^{252}Cf was performed. Thanks to the innovative design of our FIETS fission-time trigger, using the electrons ejected by the fission fragment directly from the target, an unprecedented geometrical efficiency close to 0.915% of 2π (0.784% including FIETS transmission) was achieved. The efficiency of VERDI supersedes that of the famous COSI FAN TUTTE by a factor of about 200. Moreover, FIETS allows measuring the fission fragment's time-of-flight with a minimum energy loss.

At present the pre-neutron mass resolution results in a peak-to-valley ratio of more than 60, which is 3 times larger than what is usually obtained with the double-energy technique. The structures around the maximum fragment yields are more pronounced thanks to a considerably improved mass resolution. From the comparison of our measured and simulated velocity distributions we may conclude that VERDI possesses a pre-neutron mass resolution, which is only limited by the effect of prompt neutron emission. This resolution cannot be further improved, because the underlying condition that pre-neutron and post-neutron velocities are equal is only fulfilled, when no neutron is emitted.

The post-neutron mass resolution does not yet reach the contemplated figure. This is mainly due to the limited energy resolution of the silicon detectors, which lie below expectations. The mass resolution is not easy to determine, because we deal with a distribution in mass and kinetic energy for fission fragments. From the energy resolution at α-particle energy ($\Delta E/E = 0.016$) and the known timing resolution for fission fragments of better than 0.49 ns (FWHM) the mass resolution $\Delta A/A = 0.023$ (FWHM), when assuming a minimum fission fragment TOF, i.e. maximum velocity (see Fig. 7). This may be regarded as a worst case scenario, because the energy resolution for fission fragments with high kinetic energy, i.e. low TOF, is certainly much better than that for α-particles. But it is evident from Fig. 10 that the post-neutron mass resolution degrades when going from light fragments (higher kinetic energy) to heavy fragments (lower kinetic energy).

Since we use detectors made from homogeneously doped silicon wafers, we suspect potential for improving the post-neutron mass-resolution by reducing the noise level on the pre-amplifier signals. Further limitation may come from the fact that only one FIETS assembly is presently used, limiting the quality of the time calibration on the side, where there is none. This obvious upgrade of the VERDI spectrometer is presently under way.

Finally, we show the average prompt neutron multiplicity as a function of fragment mass, $\nu(A)$, obtained from the combined pre- and post-neutron measurement. We note that the total average multiplicity turned out to be higher by about 15%. However, the features of the shape $\nu(A)$ are very well reproduced. We may, therefore, expect that in the upgraded version of VERDI prompt neutron data as a function of A, TKE and the total excitation energy will be obtained with sufficient resolution.

Acknowledgement

One of the authors (M.O.F.) is indebted to the European Commission for providing a Post-doc fellowship at the EC-JRC IRMM. We are grateful to Frederik Tovesson for his recommendations during the design of the electrostatic mirrors, and to Kaj Jansson for the careful review of the analysis code. The excellent assistance provided by N. Sevenhans and K. Okkinga in all issues related to radio-protection and the timely production of test samples by G. Sibbens, A.S.A. Rajashekar and D. Vanleeuw during the development of the FIETS detector is greatly acknowledged.

References

[1] R. Müller, A. Naqvi, F. Käppeler, F. Dickmann, Physical Review C 29 (1984) 885.
[2] A. Naqvi, F. Käppeler, R. Müller, F. Dickmann, Physical Review C 34 (1986) 218.
[3] A. Oed, P. Geltenbort, R. Brissot, F. Gönnenwein, P. Perrin, E. Aker, D. Engelhardt, Nuclear Instruments and Methods in Physics Research 219 (1984) 569.
[4] N. Boucheneb, P. Geltenbort, M. Ashgar, G. Barreau, T. Doan, F. Gönnenwein, B. Leroux, A. Oed, A. Sicre, Nuclear Physics A 502 (1989) 261c.
[5] M. Ashgar, N. Boucheneb, G. Medkour, P. Geltenbort, B. Leroux, Nuclear Physics A 560 (1993) 677.
[6] N. Boucheneb, M. Ashgar, G. Barreau, T. Doan, B. Leroux, A. Sicre, P. Geltenbort, A. Oed, Nuclear Physics A 535 (1991) 77.
[7] P. Schillebeeckx, C. Wagemans, P. Geltenbort, F. Gönnenwein, A. Oed, Nuclear Physics A 580 (1994) 15.
[8] K. Nishio, Y. Nakagome, I. Kanno, I. Kimura, Journal of Nuclear Science and Technology 32 (1995) 404.
[9] K. Meierbachtol, F. Tovesson, D. Shields, C. Arnold, R. Blakely, T. Bredeweg, M. Devlin, A. Hecht, L. Heffern, J. Jorgenson, A. LAptev, D. Mader, J. O'Donnell, A. Sierk, M. White, Nuclear Instruments and Methods in Physics Research A 788 (2015) 59.
[10] ⟨http://www.roentdek.com/products/detectors/⟩, 2015.
[11] K. Kosev, N. Nankov, M. Friedrich, E. Grosse, A. Hartmann, K. Heidel, A. Junghans, K. Schilling, R. Schwengner, M. Sobiella, A. Wagner, Detectors and Associated Equipment 594 (2008) 178.
[12] M. Frégeau, S. Oberstedt, The fission-fragment spectrometer {VERDI}, Physics Procedia 64 (2015) 197–203. (Scientific Workshop on Nuclear Fission Dynamics and the Emission of Prompt Neutrons and Gamma Rays, THEORY-3).
[13] S. Oberstedt, R. Borcea, T. Gamboni, W. Geerts, F.-J. Hambsch, R.J. Tornin, A. Oberstedt, M. Vidali, VERDI – a double (v, e) fission fragment spectrometer, In: T. Belgya (Ed.), EFNUDAT – Slow and Resonance Neutrons, 2nd Scientific Workshop on Nuclear Data Measurements, Theory and Applications, Normafa Hotel, Budapest, Hungary, 23–25 September 2009, Institute of Isotopes, HAS, 2010, p. 133, ISBN 978-963-7351-19-8.
[14] ⟨www.mesytek.com/datasheets/MSI8.pdf⟩, 2015.
[15] ⟨ww.caen.it⟩, 2015.
[16] H.W. Schmitt, W.E. Kiker, C.W. Williams, Physical Review 137 (1965) B837.
[17] A. Göök, F.-J. Hambsch, M. Vidali, Physical Review C 90 (2014) 064611.
[18] J. Velkovska, R. McGrath, Nuclear Instruments and Methods in Physics Research Section A: Accelerators, Spectrometers, Detectors and Associated Equipment 430 (1999) 507.
[19] J. Randrup, R. Vogt, Physica Review C 80 (2009) 024601.
[20] S. Whetstone Jr., Physical Review 131 (1963) 1232.
[21] C. Wagemans (Ed.), The Nuclear Fission Process, 1991.
[22] F.-J. Hambsch, S. Oberstedt, Nuclear Physics A 617 (1997) 347.
[23] T. England, B. Rider, Evaluation and Compilation of Fission Product Yields, Technical Report LA-UR-94-3106, 1993.